LATTICE BASED SIMULATION OF CHLORIDE INGRESS IN UNCRACKED AND CRACKED CONCRETE: MODEL VALIDATION

BRANKO ŠAVIJA[*], JOSE PACHECO[*] AND ERIK SCHLANGEN[*]

[*] Delft University of Technology
Stevinweg 1, 2628 CN Delft, the Netherlands
e-mail: b.savija@tudelft.nl; j.pachecofarias@tudelft.nl; h.e.j.g.schlangen@tudelft.nl, www.tudelft.nl

Key words: Durability, Chlorides, Cracking, Lattice Model

Abstract: Reinforced concrete structures are frequently exposed to aggressive environmental conditions. Most notably, chloride ions from sea water or de-icing salts are dangerous for the reinforcement. Good concrete cover can ensure its protection. However, it is necessary to study the effects of material heterogeneity and cracking on chloride ingress in concrete. This is done herein by proposing a three-dimensional lattice model capable of simulating chloride transport in saturated sound and cracked concrete. Means of computationally determining transport properties of individual phases in heterogeneous concrete (aggregate, mortar, and interface), knowing the concrete composition and its averaged transport properties, are presented and discussed. Based on numerical experimentation and available literature, a relation between the effective diffusion coefficient of cracked lattice elements and the crack width was adopted. Finally, these findings were validated on experimental results from the literature and discussed.

1 INTRODUCTION

Modern reinforced concrete structures, if properly designed and executed, can achieve their intended service life. Corrosion of reinforcing steel due to chloride ingress can be prevented. An increasing number of service life models are available to aid the practicing engineer. These are all based on one, but very crucial, assumption: that the structure in question is and remains crack free. Evidently, this is almost never the case: reinforced concrete structures crack due to many reasons, most important ones being mechanical loading and shrinkage. This has been an issue of increasing focus in the research community lately: a number of publications deals with experimental investigations on the influence of cracking on chloride ingress (see [1]) and reinforcement corrosion (see [2]) in cracked concrete.

Apart from experimental studies on the subject, a number of models have been proposed in the literature. Some of them model the effect of cracking in a smeared way, by introducing an increase of the diffusion coefficient in the whole domain (e.g. [3]). Others model cracks as notches or faults in concrete, without the mechanical analysis (e.g. [4, 5]). Very few have made a step further, and coupled the mechanical and transport analyses (e.g. [6]). Most of these models treat concrete as a quasi-homogeneous continuum, i.e. mechanical and transport properties are constant for the whole domain. On the other hand, a truss-network approach proposed by [7], considers concrete as a three-phase composite, consisting of coarse aggregate, mortar, and ITZ. Both of these approaches (homogeneous and heterogeneous) are applicable within the lattice framework as presented here.

In the following, a three dimensional lattice

model for simulating chloride penetration in sound and cracked concrete is presented. Governing equations and discretization procedure are only briefly addressed. The focus of the paper lies on determination of transport properties of different phases in concrete (aggregate, mortar, and the interface), and cracks. The model is validated using experimental results from the literature. Finally, these results are discussed and evaluated, and some conclusions are drawn.

2 METHOD

2.1 Model description

Lattice models have long been used in fracture mechanics of concrete [8]. Recently, the use of lattice (or rather discrete) models has been extended on simulating transport processes in concrete [7, 9, 10]. Coupling of the mechanical and transport simulations, while taking into account the effect of cracking on the transport mechanism, was performed by [10, 11]. In the mechanical lattice approach, concrete is discretized as a set of truss or beam elements. In the transport lattice approach, concrete is treated as an assembly of one-dimensional "pipes", through which the flow takes place. While some authors use "dual" lattices (one for the mechanical simulation, and the other for the flow simulation- for details see [11]) the approach proposed here uses the same lattice network for both simulations. In this approach, mechanical simulation is performed first; its output is then used as an input for simulating chloride ingress. Therefore, it is actually a one-way coupling - mechanical degradation does effect the chloride penetration, while, on the other hand, there is no influence of the chloride penetration on the mechanical behavior.

In order to take material heterogeneity into account, the particle overlay procedure (schematically shown in figure 1) is employed: it is in this manner that different transport (or mechanical) properties are assigned to different phases. For this purpose, either a computer-generated material structure, or a

material structure obtained by micro-CT scanning can be used. What has to be noted here is that interface, as used in the present model, does not exactly coincide with the interfacial transition zone (ITZ). Its thickness is between 30 and 80μm [12], while on the other hand interface elements in the present model take up also a piece of aggregate and a piece of mortar (figure 1). Their actual size in the model depends on the characteristic element size. Therefore, the transport properties of this "phase" are slightly altered, as explained later.
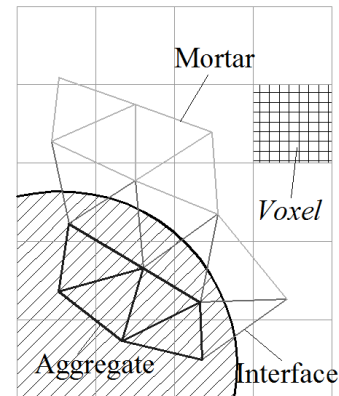

Figure 1: Particle overlay procedure (2D)

Saturated concrete was assumed in all analyses, since the purpose of this work was to validate the approach by comparing the results with experimental data, not to develop a fully functional service-life modelling tool. Therefore, Fick's second law was assumed to be valid, and diffusion was the only transport mechanism considered.

2.2 Phase transport properties

In order to determine transport properties of individual phases within the heterogeneous concrete, the approach developed by [13] (the so-called n-phase model) was used. The model was developed with spherical particles in mind, so for any other particle shape (e.g. the Anm material model developed by [14]) can be considered as only an approximation. The following formulae were used (assuming impermeable aggregates):

$$D_{eff}/D_M = N/D \qquad (1)$$

Here, the following are:

$$N=6D_M(1-C_A)(C_A+C_I)$$
$$+2C_I(D_I-D_M)\cdot(1+2C_A+2C_I)$$

$$D=3D_M(2+C_A)(C_A+C_I) \qquad (2)$$
$$+2C_I(1-C_A-C_I)(D_I-D_M)$$

Here, D_{eff}, D_M, and D_I are the effective diffusion coefficient of concrete, the diffusion coefficient of the mortar phase, and the diffusion coefficient of the interface phase, respectively. Also, C_A and C_I are volume fractions of the aggregate and the interface phases, respectively. This approach enables one to determine the diffusion coefficient of individual phases (mortar and interface) in concrete, given the volumetric contents of each phase, and the effective diffusion coefficient of concrete. All these are usually available from the experimental data. Therefore, in order to determine this, it is necessary to determine the ratio between the diffusion coefficient of mortar and the diffusion coefficient of the interface.

To estimate the magnitude of this relation, a set of experimental data provided by [15] was used. Here, transport properties of concrete are compared to corresponding mortars. Concrete used in the experiments contained about 35% coarse aggregate by volume. Rapid chloride migration test was used in order to determine the non-steady state migration coefficient (D_{NSSM}) of concretes and mortars. From these, diffusion coefficients (D) were calculated.

Table 1: Results of [15] (C-concrete, M-mortar)

ID[*]	D_{NSSM} ($\cdot 10^{-12}$ m^2/s)			D ($\cdot 10^{-12}$ m^2/s)		
	C	M	M/C[†]	C	M	M/C[†]
NI0	6.56	8.80	1.34	2.43	5.53	2.28
NIF15	3.54	4.55	1.29	1.47	3.18	2.17
NIS15	5.77	6.79	1.18	2.16	4.31	2.00
NIS30	5.42	4.93	0.91	2.00	3.09	1.54
NV0	9.43	11.94	1.27	3.35	7.20	2.15
NVF30	3.43	5.04	1.47	1.19	2.94	2.47
NVS30	4.68	5.49	1.17	1.70	3.39	2.00
LI0	15.7	11.23	0.71	5.48	6.64	1.21
HI0	3.76	5.4	1.44	1.49	3.56	2.40
HIS30	3.54	2.92	0.82	1.42	1.96	1.37

[*] Different concrete/mortar mix designs from [15]

[†] Not provided in [15]

By careful observation of the results, it is clear that the ratio of mortar to concrete diffusion coefficient (M/C) changes dramatically when the diffusion coefficients are calculated. It even states that, in some cases, the diffusion coefficient of mortar is higher than that of concrete, even though its non-steady state migration coefficient is lower. This is hardly to be the case. In order to correct this, diffusion coefficients of concrete were calculated using a suggestion from [16]: it is stated that there exists a linear relationship between the non-steady state migration coefficient (D_{NSSM}) and the diffusion coefficient of concrete (D). Similarly, [17] found that there is a linear relationship between the non-steady state diffusion coefficient obtained from the accelerated chloride migration test (ACMT), and the diffusion coefficient obtained from the ponding test, irrespective of the concrete composition. Linear regression of the data provided by [16] yields the following equation:

$$D=0.9672\cdot D_{NSSM}-2.6389 \qquad (3)$$

where D and D_{NSSM} are in 10^{-12} m^2/s. Furthermore, by employing the M/C ratio from the migration experiment, the diffusion coefficient of mortar is calculated. It has to be noted that equation (3) is used here merely as a tool to calculate the diffusion coefficient from the non-steady state migration coefficient.

Table 2: Calculated diffusion coefficients

	D ($\cdot 10^{-12}$ m^2/s)		
ID	C	M	D_I/D_M
NI0	3.70	4.97	2.79
NIF15	0.78	1.01	3.06
NIS15	2.94	3.46	3.57
NIS30	2.60	2.36	5.23
NV0	6.48	8.21	3.14
NVF30	0.68	1.00	2.24
NVS30	1.88	2.21	2.46
LI0	12.56	8.98	7.16
HI0	1.00	1.44	2.39
HIS30	0.78	0.65	5.94

In order to determine the ratio between the

diffusion coefficient of mortar and the diffusion coefficient of the interface (D_I/D_M ratio), a concrete material structure with about 35% of coarse (spherical) aggregates was generated using a simple packing algorithm. A lattice with characteristic elements size (voxel size) of 1 mm was projected on top of it, and volume of lattice elements of each phase was calculated (58.41% mortar, 29.35% aggregate, and 12.24% interface). Then, using formulae (1) and (2), the ratio between the diffusion coefficient of mortar and the diffusion coefficient of the interface was calculated for each mixture (Table 2). In order to achieve the desired effective concrete properties, these vary in the range 2.24-7.16. This seems to be in accordance with the variability of the diffusion coefficient of ITZ, which is stated to be somewhere in the range 2-8 times that of the cement paste [12].
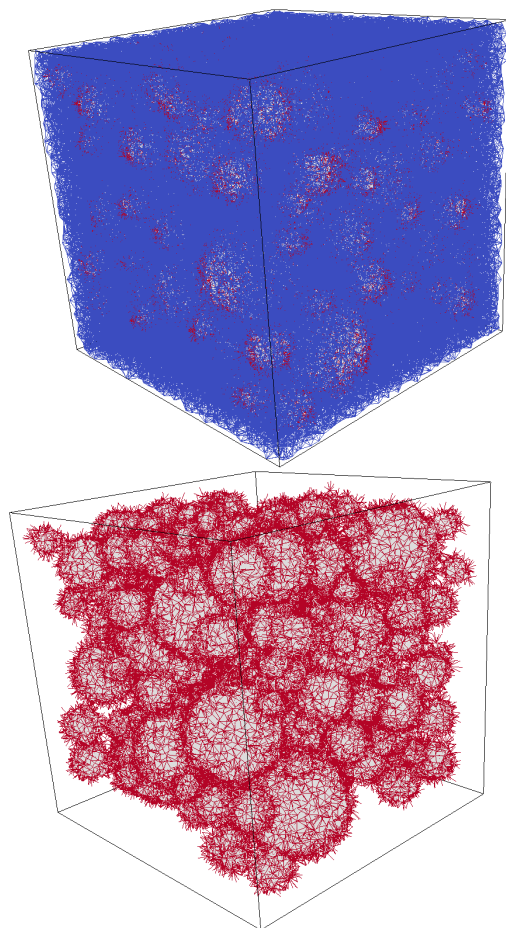
Figure 2: Determination of the D_I/D_M ratio (top-the whole lattice; bottom-only aggregate and the interface)

The variability of this parameter can also be

taken into account in a statistical manner; however more experimental results are needed to justify this approach. Based on presented analysis, a deterministic value of 3 for the D_I/D_M ratio was selected. This value is used in further analyses.

2.3 Crack transport properties

Two sets of experiments performed by Ismail et al. [18, 19] are used for determining transport properties of a single crack. They used the expansive core method to create parallel-walled cracks in doughnut shaped specimens. Due to a large variety of smaller crack widths, these experiments are suitable for the procedure employed here. First set of experiments [18] was performed on cracked brick samples, while the second set [19] used cracked mortar samples. In both instances, cracked samples were placed in a chloride penetration cell, with chloride loading on both sides of the sample. After the exposure period, using the grinding technique, two types of chloride profiles were determined: perpendicular to the exposed surface, and perpendicular to the crack walls. The second type of profiles were determined by grinding the material in the middle part of the specimen height, in order to ensure that powder samples would contain only chloride ions penetrating from the crack plane, and not from the sample surface (figure 4).
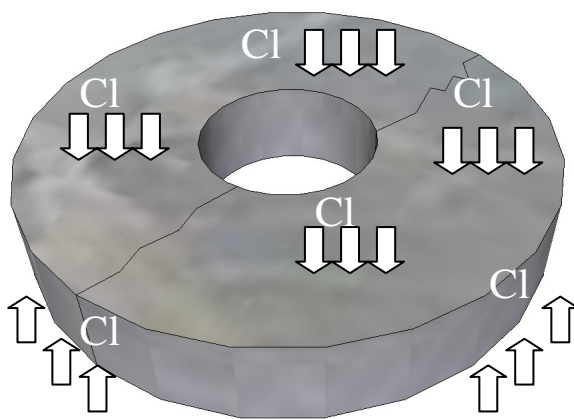

Figure 3: Brick/mortar specimen of [18, 19]

Here, the approach proposed by [7] was used. In order to determine the effective crack transport properties, numerical simulation

4

results are fitted to experimental data. To simplify the process, the mechanical analysis is not performed here; rather an artificial "crack" with varying transport properties (corresponding to different crack widths) is created in the middle of the analysed specimen, and simulation results compared to experiments. For the simulations, a 3D slice of 50×5×50 mm was used, with a total number of 12500 nodes and 85095 lattice elements.
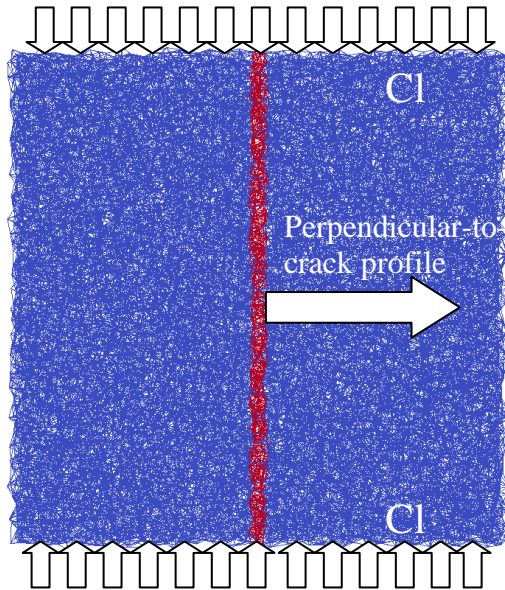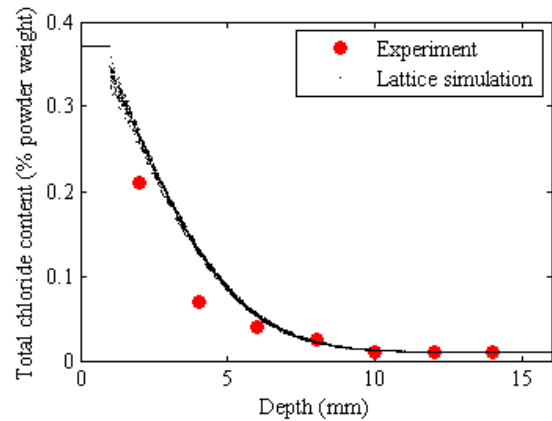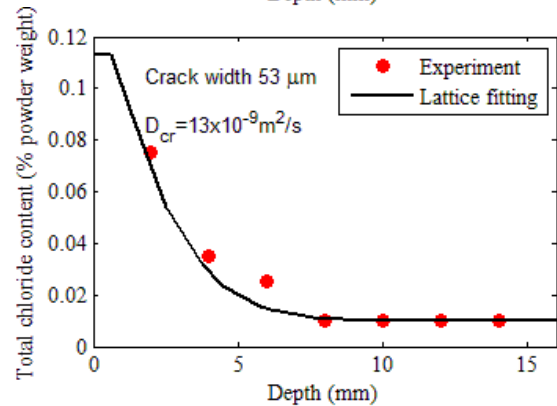
different crack widths are shown in figure 6.

Figure 5: Surface chloride profile-uncracked sample (brick)

Figure 4: Lattice used in the simulations. Blue-brick/mortar, red-"crack"

First, experimental results of cracked brick specimens are reproduced [18]. After cracking, these were fitted in the chloride penetration cell, and exposed for 10 hours. Regression analysis of the chloride profile perpendicular to the exposed surface (uncracked sample) yielded the diffusion coefficient of $156.71 \cdot 10^{-12}$ m^2/s, and the surface chloride concentration of 0.37% per weight of sample (figure 5). These were used as input for all analyses of this experiment.

In order to obtain results close to experimental values, a trial-and-error procedure was followed. This means that the effective diffusion coefficient of "cracked" elements was adjusted until the calculated perpendicular-to-crack profile corresponded well to the experimental one. Values of the fitted effective diffusion coefficients for
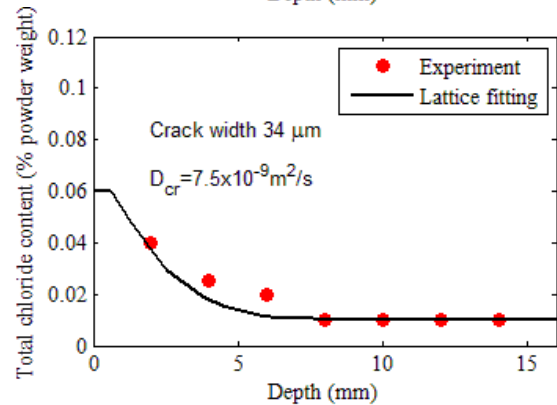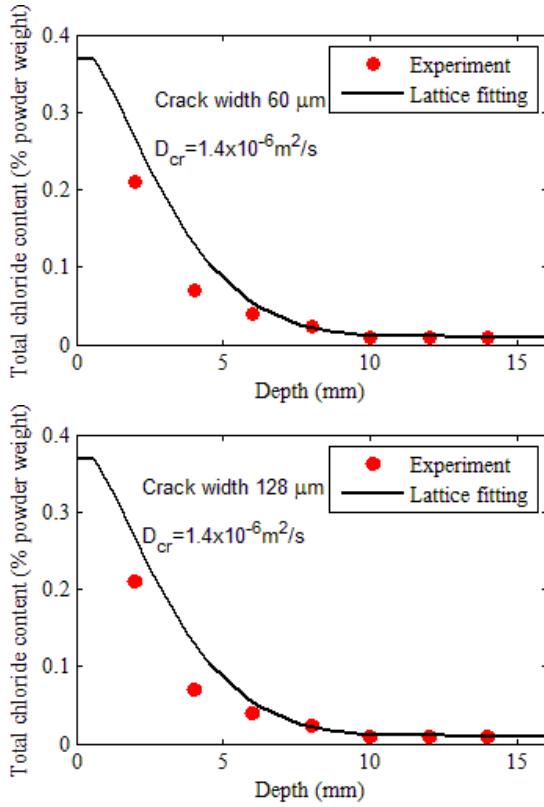
Figure 6: Perpendicular-to-crack chloride profiles for different crack widths (brick)

For large cracks (60μm and 128μm), the effective diffusion coefficient is 3 orders of magnitude higher than the diffusion coefficient of chloride ions in free bulk water (which is around $2.03 \cdot 10^{-9}$ m^2/s at 20°C [20]). These results seem to be in good accordance with values proposed by [7]. They also suggested that the effective diffusion coefficient in large cracks is very large, much higher than that in free bulk water. This was attributed to additional transport mechanisms which may occur in the crack, e.g. "convection current due to the small temperature gradient and/or small hydraulic pressure gradient". However, it is also possible that the brick specimens had not been fully saturated when the experiment begun, so capillary suction might have played a significant role. Due to high porosity of brick samples, this could strongly influence the chloride ingress behaviour. Based on the present tests, the following quadratic relation can be proposed:

$$D_{CR}=10^{-6} \cdot (4.2384 \cdot 10^{-6} w^2 - 7.926 \cdot 10^{-5} w + 0.0052954),$$
$$\text{for } w \leq 55 \ \mu m$$
$$D_{CR}=1.4 \cdot 10^{-6}, \qquad (4)$$
$$\text{for } w > 55 \mu m$$

The value of 55μm in (4) was selected based on the recommendation of [18]. It was found, after performing a deformation-controlled uniaxial tension test on the material, that the critical crack opening of about 50-55μm is where the mechanical interaction between crack surfaces ceases to exist, so there can be no reduction of the chloride diffusion in larger cracks. This value is higher for concrete, where, due to material heterogeneity, crack bridging also occurs.

In order to check whether these results are directly applicable to cement based materials, the same experiment, but this time on cracked mortar samples, was simulated [19]. In this work, two series of mortar specimens were cracked at different ages (28 days and 2 years). These were tested in order to check also the influence of cracking age on autogeneous healing of cracks. Regression analyses of perpendicular-to-surface profiles yielded the following data: diffusion coefficient of $8.66 \cdot 10^{-12}$ m^2/s, surface chloride concentration of 0.32% mortar weight; and the diffusion coefficient of $7.51 \cdot 10^{-12}$ m^2/s, surface chloride concentration of 0.32% mortar weight, for 28 days and 2 years series, respectively. In both instances, specimens were exposed to chloride loading for a total of 14 days.

Based on (4), effective diffusion coefficients for different crack widths were calculated. After the analyses were performed, the results indicated that (4) overestimated the perpendicular-to-crack diffusion in cracked mortar (figure 7). A different relation [21] was also used to check whether it gives better results when applied to cement-based materials:

$$D_{CR}=2 \cdot 10^{-11} w - 4 \cdot 10^{-10},$$
$$\text{for } 30 \mu m \leq w < 80 \mu m$$

6

$$D_{CR} = 1.4 \cdot 10^{-9}, \qquad (5)$$

$$For\ w \geq 80 \mu m$$

The lower bound in the equation accounts for crack healing (30μm). The upper bound (80μm) is where mechanical interaction between the crack faces ceases to exist (higher for concrete than for brick-see (4)).

Comparison of the simulations performed with use of both (4) and (5) is shown in figure 7. Note that (5) was used here also for a crack narrower than 30μm (29μm in this case), which was created in mortar after 2 years. Unlike the specimens cracked at a young age, these older specimens have a diminished autogeneous healing potential. This is due to the fact that the amount of unhydrated cement is low in these samples.
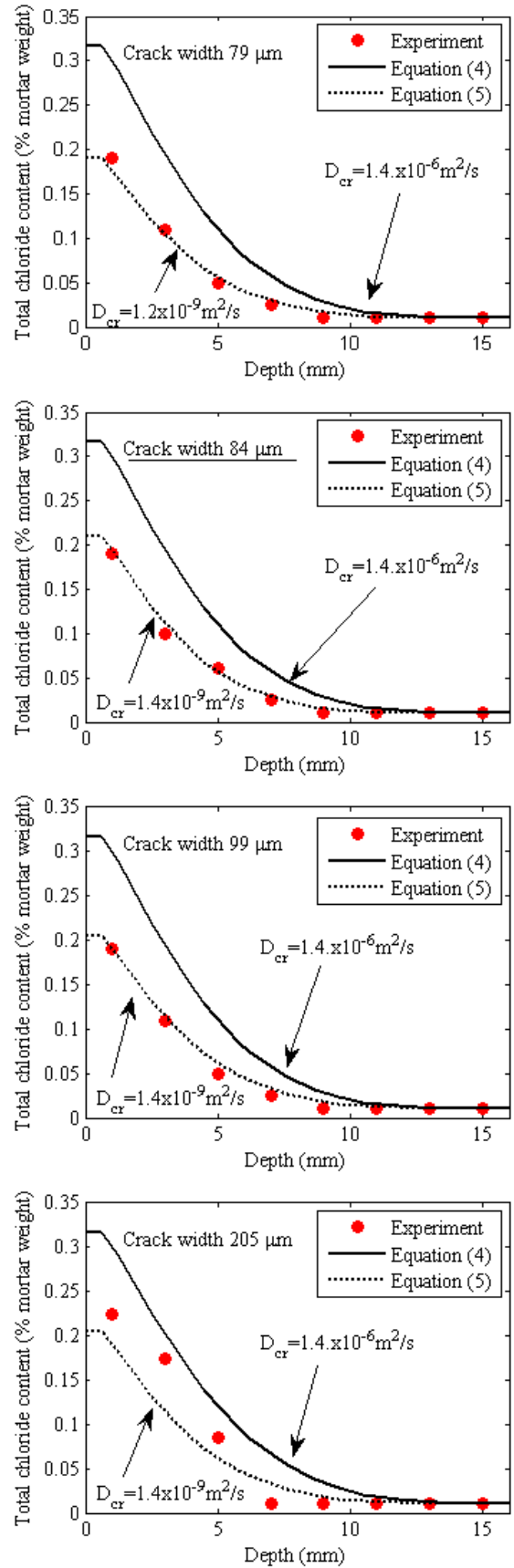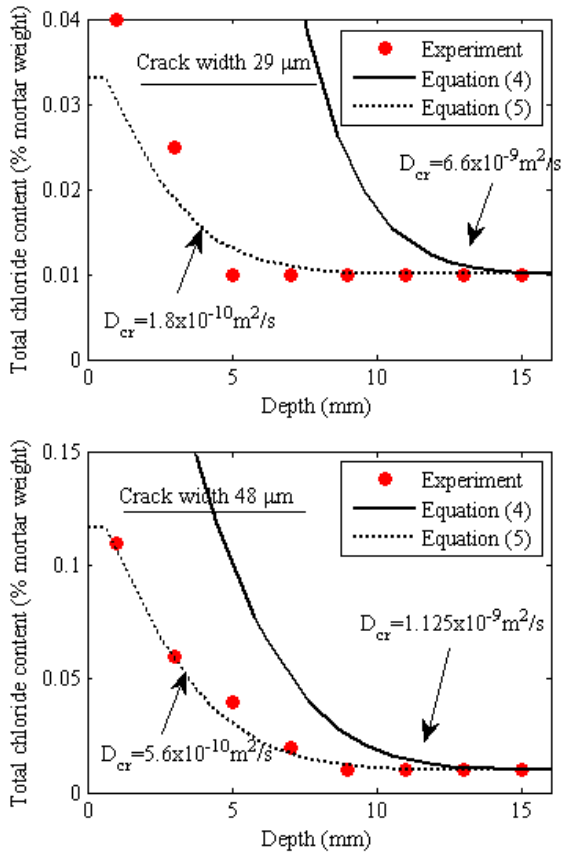

Figure 7: Perpendicular-to-crack chloride profiles for different crack widths (mortar). Not underlined-cracked

at 28 days. Underlined- cracked at two years.

Clearly, the values obtained from equation (4) overestimate the perpendicular-to-crack chloride penetration in this case. On the contrary, results obtained using (5) are in good agreement with the experiments. It seems, then, that the values which hold for cracked brick specimens overestimate the chloride penetration in cracked mortar. Since brick is much more brittle and homogeneous, no crack branching and bridging occurs when it cracks. This potentially slows down chloride ingress through cracks in heterogeneous materials, like mortar and concrete. Also, it is most probable that capillary suction played a significant role in [18], thereby altering the effective transport properties of a crack. Also, whether results from tests on different materials can be applied directly to mortar and concrete is questionable. In the mechanical lattice model with embedded aggregate particles, crack branches and bridges will be found automatically, and slowing down the diffusion process. It can be, therefore, concluded that equation (5) can be used to simulate chloride penetration in cracked cement based materials using the proposed lattice approach.

3 VALIDATION AND DISCUSSION

3.1 Heterogeneous material

In order to validate the approach developed in chapter 2.2, experimental data provided by [17] was used. A 90-day ponding test was used to determine the diffusion coefficient of different concretes. All concrete mixes used in their study had a volumetric content of coarse aggregates of about 30%., with maximum grain size of 10mm. For the simulation, a concrete material structure with about 30% of coarse aggregate particles was generated. A lattice with characteristic elements size (voxel size) of 1 mm was projected on top of it, and volume of lattice elements of each phase was calculated (61.60% mortar, 22.50% aggregate, and 15.90% interface). The total size of the mesh was 50×50×50mm, with 125000 nodes and 938156 lattice elements. This particular mix was made using ASTM Type I Portland

cement as a binder.

Regression analysis of experimental data yielded the following: diffusion coefficient of $47.614 \cdot 10^{-12}$ m^2/s, and surface chloride content of 0.51%. Using equations (1) and (2) and the D_I/D_M value of 3, diffusion coefficients of the mortar and the interface phases were calculated as $48.35 \cdot 10^{-12}$ m^2/s, and $145.06 \cdot 10^{-12}$ m^2/s, respectively.

An analysis was performed using both the homogeneous and the heterogeneous lattices, using the input data as provided above.

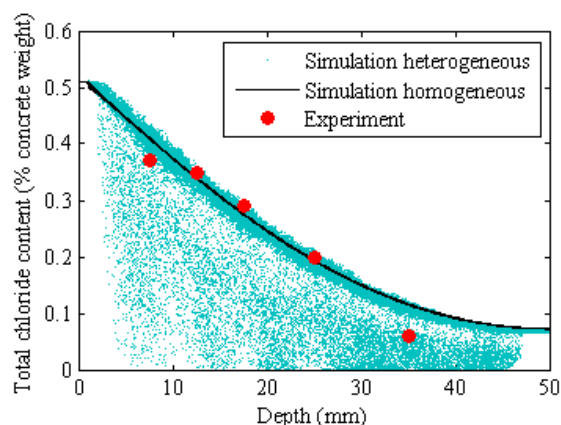**Figure 8:** Comparison of the homogeneous and heterogeneous lattice analyses and the experiment
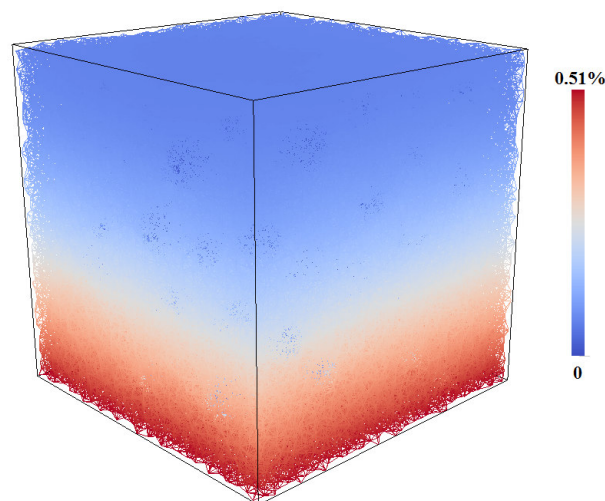

Figure 9: Total chloride content from the heterogeneous analysis (% of concrete weight)

Figure 8 shows that the results of both homogeneous and heterogeneous lattice analyses correlate well with experimentally obtained data. Zero values in the heterogeneous lattice analysis correspond to lattice nodes which are inside the impermeable

aggregate particles; therefore, no chloride ions can be present. Other points below the maximum penetration band show that, in a heterogeneous material as modelled here, there is no sharp front of chloride penetration. Instead, a three-dimensional profile is present, with variable chloride content at a certain depth. It can also be seen that there exists a difference between the maximum total chloride content at a certain depth (the one obtained from the heterogeneous analysis), and the value which is obtained if concrete is considered to be a homogeneous medium. By performing similar analyses (but considering concrete as a two-phase medium, comprising mortar and coarse aggregates), this phenomenon also occurred in other studies [22, 23]. They suggested that this could be one of the factors contributing to large discrepancy in values of critical chloride contents reported in the literature. It is possible that a threshold value of chloride is reached in certain points on the reinforcing steel, thus depassivating it and creating local corrosion pits. However, chloride content elsewhere along the steel could be lower, due to material inhomogeneity. Due to the usual experimental procedure (i.e. grinding the material close to the reinforcing steel and performing chemical analysis to determine the chloride content), the value obtained would be lower than the actual value which caused the local depassivation of the steel. This phenomenon justifies the use of more advanced material models, such as the presented one, in order to get more insight into the process of steel depassivation and corrosion pit locations in concrete. Also, it encourages the use of more sophisticated experimental techniques, such as laser-induced breakdown spectroscopy (LIBS) [24] or electron probe microanalysis (EPMA) [25], especially when determining the value of critical chloride content in concrete.

3.2 Cracked material

The approach presented in chapter 2.3. was verified on experimental results of [26]. Mortar prisms (355.6×50.8×76.2mm) reinforced with three levels of steel mesh reinforcement were cast. The prisms were reinforced to enable creation of varying controlled widths. After the curing period, they were cracked using 4-point bending test to obtain different crack widths. After loading, one single crack occurred in each of the specimens. Cracks formed in bending are tapered (V-shaped). Upon unloading, some crack closure occurred, so their width was measured in the unloaded state. Then, the samples were exposed to NaCl solution for 30 days. After the exposure period, area around the crack was drilled, ground, and analyzed for chloride.

Regression analysis of the experimental data gave the following (for the uncracked sample): diffusion coefficient of $20.3 \cdot 10^{-12}$ m^2/s, and surface chloride content of 0.39% by weight of mortar. The analyzed sample had a size of 355×50×75mm, with a characteristic element size of 2.5mm. Steel mesh reinforcement was neglected in the simulation. First, a mechanical analysis was performed. Using a four-point bending setup, cracks of different widths were produced. As in the experiments, one single crack formed in the fracture analysis. The output of the mechanical analysis was used as input for the chloride diffusion analysis. Equation (5) was used for defining the effective diffusion coefficients of cracks. Every "local" cracked element has its own value of the diffusion coefficient, depending on its crack width.
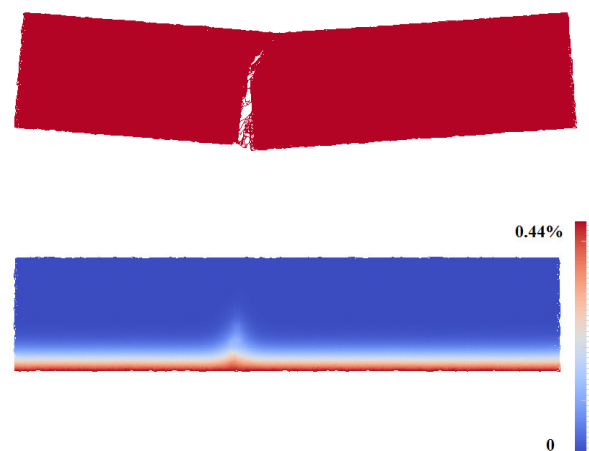

Figure 10: Mortar sample with surface crack width of 369μm. Top- crack pattern. Bottom- total chloride

profile (% of mortar weight) after 30 days of exposure.

Several analyses were performed using the range of surface crack widths similar to the experiments. The surface chloride contents for each analysis were adjusted to match those in experiments with a similar crack width. Both experimental and simulation results are shown in figure 11.
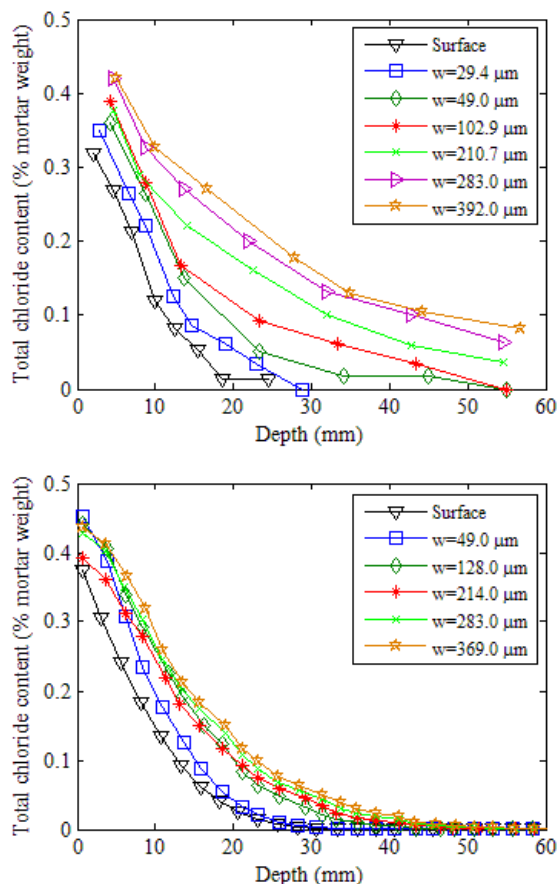

Figure 11: Total chloride profiles for different crack widths after 30 days of exposure. Top- experiment; bottom- simulation.

As expected, chloride penetration depth increases with the increase of surface crack width. The effect is less pronounced than in the case of a parallel-walled crack, though. This is due to the fact that bending cracks are V-shaped, being wider at the surface than on the inside of the prism. According to equation (5), cracks wider than 80μm all have the same effective diffusion coefficient. However, since wider bending cracks also run deeper, the effect of widening is still pronounced with large cracks. This means that widening of the

cracks above the 80μm threshold does increase chloride penetration further, since they become deeper in the process.

Comparing the experimental and simulation results (figure 11), evidently there is a difference. Experimental results for wider cracks (more than 210μm) show a more pronounced influence of cracking, compared to simulation results. There are two reasons for this: first, the crack width was measured in the unloaded state. This means that the crack was larger during the loading and some damage was created, which is not accounted for in the model. Secondly, some cracks have probably formed alongside the steel mesh reinforcement, speeding up the lateral chloride penetration. This was disregarded in the model. Overall, the simulation results seem to be in relatively good agreement with experimental data. Accordingly, the approach developed in chapter 2.3 can be successfully employed in simulating chloride ingress in cement based materials cracked in flexure.

4   SUMMARY AND CONCLUSIONS

As cementitious materials are highly inhomogeneous and cracked, their transport properties show significant local variations. More advanced models than presently available are needed for studying these effects. In view of this, a three-dimensional lattice model for simulating chloride ingress was developed. The proposed framework described here enables:

(1) Simulating chloride ingress in heterogeneous concrete, i.e. taking into account the presence of impermeable aggregate particles and porous interface surrounding them.

(2) Taking into account presence of cracks on chloride ingress, by coupling the simulation with the mechanical analysis.

In order to focus on these two issues, saturated concrete was assumed in all analyses.

The procedures developed were tested and validated using data from the available literature. The following conclusions can be reached from the presented numerical simulations:

(1) When neglecting the material heterogeneity, simulation results are very close to experimental ones. The reason for this lays in the usual experimental procedure (grinding and chemical titration), which gives an averaged value of the chloride content at a certain depth.

(2) The heterogeneous model shows some deviation from the perfect diffusion profile, which is commonly observed in experiments where penetration depth is determined by silver nitrate spraying. More importantly, maximum chloride contents at a certain depth are higher than the averaged ones. This should be kept in mind, especially when studying the critical chloride content in concrete. Use of more advanced experimental methods is therefore encouraged.

(3) Mechanical cracks do promote chloride ingress into concrete, depending on their width. This is observed also in the model. However, even though commonly addressed only by their surface widths, not all cracks are created equal. Bending cracks are V-shaped, meaning that a part of the crack close to its tip remains inaccessible for rapid chloride penetration. Accordingly, parallel walled cracks of certain surface width are more detrimental than flexural cracks of the same surface crack width. Coupling of the mechanical and transport model, as proposed here, enables studying this behaviour in more detail.

Finally, it can be concluded that the presented model can be successfully employed in simulating chloride penetration in both sound and cracked cement based materials. Presence of coarse aggregates in concrete can be included in the model, and gives more insight on the transport behaviour.

ACKNOWLEDGEMENTS

REFERENCES

[1] Šavija, B. and Schlangen, E., 2012. Chloride ingress in cracked concrete-a literature review. In Andrade and Gulikers (eds.), *Advances in Modeling Concrete Service Life*, pp. 133-142, Springer

[2] Pacheco, J. and Polder, R.B., 2012. Corrosion initiation and propagation in cracked concrete-a literature review. In Andrade and Gulikers (eds.), *Advances in Modeling Concrete Service Life*, pp. 85-93, Springer

[3] Rahman, M.K., Al-Kutti, W.A., Shazali, M.A. and Baluch, M.H., 2012. Simulation of chloride migration in compression-induced damage in concrete. *J Mater Civil Eng* **24**(7):789-796

[4] Boulfiza, M., Sakai, K., Banthia, N. and Yoshida, H., 2003. Prediction of chloride ions ingress in uncracked and cracked concrete. *ACI Mater J* **100**(1):38-48

[5] Adiyastuti, S.M., 2005. *Influence of cracks on chloride induced corrosion in reinforced concrete structural members*, PhD Thesis, University of New South Wales, Sydney, Australia

[6] Ožbolt, J., Balabanić, G., Periškić, G., Kušter, M., 2010. Modelling the effect of damage on transport processes in concrete. *Constr Build Mater* **24**:1638-1648

[7] Wang, L. and Ueda, T., 2011. Mesoscale modelling of the chloride diffusion in cracks and cracked concrete, *J Adv Concr Technol*, **9**(3):241-249

[8] Schlangen, E., 1993. *Experimental and numerical analysis of fracture processes in concrete*, PhD Thesis, Delft University of Technology, Delft, the Netherlands

[9] Sadouki, H. and van Mier, J.G.M., 1997. Meso-level analysis of moisture flow using a lattice-type approach. *Mater Struct* **30**:579-587

[10] Bolander, J.E. and Berton, S., 2004. Simulation of shrinkage induced cracking in cement composite overlays. *Cement Concr Comp* **26**: 861-871

[11] Grassl, P., Fahy, C., Gallipoli, D. and Bolander J.E., 2012. A lattice model for

fracture and mass transport in concrete. In Ye et al. (eds.), *Second International Conference on Microstructural-related Durability of Cementitious Composites*, April 11-13, 2012, Amsterdam, the Netherlands

[12] Delagrave, A., Bigas, J.P., Ollivier, J.P., Marchand, J. and Pigeon, M., 1997. Influence of the interfacial zone on the chloride diffusivity of mortars. *Adv Cem Based Mater* **5**(3-4):86-92

[13] Caré, S. and Hervé, E., 2004. Application of a n-phase model to the diffusion coefficient of chloride in mortar. *Transport Porous Med* **56**(2):119-135

[14] Qian, Z., 2012. *Multiscale modeling of fracture processes in cementitious materials*, PhD Thesis, Delft University of Technology, Delft, the Netherlands

[15] Oh, B.J. and Jang, S.Y., 2004. Prediction of diffusivity of concrete based on simple analytic equations. *Cement Concrete Res* **34**:463-480

[16] Tang, L. et al., 2005. Guideline for Practical Use of Methods for Testing the Resistance of Concrete to Chloride Ingress, *EU-Project CHLORTEST, Project No: G6RD-CT-2002-00855*

[17] Yang, C.C. and Wang, L.C., 2004. The diffusion characteristic of concrete with mineral admixtures between salt ponding test and accelerated chloride migration test. *Mater Chem Phys* **85**:266-272

[18] Ismail, M., Toumi, A., François, R. and Gagne, R., 2004. Effect of crack opening on the local diffusion of chloride in inert materials. *Cement Concrete Res* **34**:711-716

[19] Ismail, M., Toumi, A., François, R. and Gagne, R., 2004. Effect of crack opening on the local diffusion of chloride in cracked mortar samples. *Cement Concrete Res* **38**:1106-1111

[20] Hill, D., 1984. Diffusion coefficients of nitrate, chloride, sulphate and water in cracked and uncracked Chalk, *J Soil Sci* **35**(1):27-33

[21] Djerbi, A., Bonnet, S., Khelidj, A., Baroghel-Bouny, V., 2008. Influence of traversing crack on chloride diffusion into concrete. *Cement Concrete Res* **38**:877-883

[22] Yu, H. and Hartt, W.H., 2011. Modeling corrosion initiation of reinforcing steel in concrete: effect of non-diffusive coarse aggregate. *J Compos Mater* **45**(2):153-169

[23] Soive, A. and Baroghel-Bouny, V., 2012. Influence of gravel distribution on the variability of chloride penetration front in saturated uncracked concrete, *Construct Build Mater* **34**:63-69

[24] Weritz, F., Schaurich, D., Taffe, A. and Wilsch, G., 2004. Effect of heterogeneity on the quantitative determination of trace elements in concrete. *Anal Bioanal Chem* **385**(2):248-255

[25] Win, P.P., Watanabe, M. and Machida, A., 2004. Penetration profile of chloride ion in cracked reinforced concrete. *Cement Concrete Res* **34**:1073-1079

[24] Şahmaran, M., 2007. Effect of flexure induced transverse crack and self-healing on chloride diffusivity of reinforced mortar. *J Mater Sci* **42**:9131-3196